

spectra upon reduction (occupation of the  $b_{1u}$  orbital; cf. Chart IV); complete analyses of these complicated spectra will be reported elsewhere.<sup>37</sup>

In agreement with the MO calculations (Table I), the dinuclear anion radical complex  $(4,4\text{-apy}^{\cdot-})[\text{W}(\text{CO})_5]_2$  displays a more complex ESR spectrum because the unpaired electron is now distributed over more nonequivalent CH and N  $\pi$  centers (Chart IV). The inherently broad lines of  $\text{W}(\text{CO})_5$ -containing anion radicals<sup>13,20a,d,35</sup> and the generally very strong anisotropic line broadening of outer ( $m_N \pm 2$ ) azo nitrogen ESR components<sup>34</sup> have impaired the hyperfine analysis; Table III summarizes the data as obtained from computer-simulated spectra (Figure 5) that are compatible with the HMO-McLachlan-calculated<sup>24c</sup> spin populations. This type of calculation does not take into account the nonequivalence of CH(pyridyl) centers that results from the slow rotation around the "single" bonds between azo and aromatic groups;<sup>34</sup> the bond order increase of such single bonds connecting coplanar  $\pi$  systems is a common phenomenon.<sup>13</sup>

A large LUMO/SLUMO energy difference (Figure 1), considerable spin density at the  $\text{W}(\text{CO})_5$ -coordinating pyridine nitrogen centers (Chart IV, Tables I and III), and the large spin-orbit coupling factor of  $\text{W}(0)$ <sup>36</sup> combine to cause a significant increase of  $g$  upon coordination of the carbonylmetal fragments to the 4,4'-apy anion radical (Table III).<sup>11c,13,20d,35</sup> The <sup>183</sup>W coupling constant should be around 0.09 mT according to an established<sup>20d</sup> relation  $a(^{183}\text{W}) = 0.333a(^{14}\text{N}) + 0.013$  mT for

(37) Matheis, W.; Kohlmann, S.; Kaim, W. Unpublished results.

similar systems; such a small isotope splitting could not be detected here because of the complexity of the spectrum and the broadness of individual lines.

**Outlook.** According to their MO characteristics and basic experimental data, the two new conjugated bridging ligands differ markedly from the systems used hitherto (Charts I-III). Although these two new systems offer very low-lying  $\pi^*$  levels for back donation and reduction, the small or even vanishing 4,4'-bptz LUMO coefficients  $c_N^2$  at the basic, sterically unhindered pyridine coordination centers should result, e.g., in small  $E_{\text{com}}$  values for mixed-valence systems<sup>32</sup> and relatively low intensities of MLCT absorption bands.<sup>15</sup> The small amount of spin density transferred to the metal fragments should also reduce the substitutional labilization of carbonyl ligands upon reduction<sup>33b</sup> because the  $\delta$  in the  $(18 + \delta)$  valence electron formulation for the anion radical complexes is now very small and the absolute reduction potentials are not too negative.<sup>38</sup> Coordination-induced orbital crossing  $a_u/b_{1u}$  remains a possibility to be explored for the 4,4'-bptz system; this special situation and the effects of the additional azo coordinating centers on the excited state properties are currently being studied.<sup>22</sup>

**Acknowledgment.** This work was generously supported by the Deutsche Forschungsgemeinschaft and the Stiftung Volkswagenwerk.

(38) Gross-Lannert, R.; Kaim, W.; Lechner, U.; Roth, E.; Vogler, C. Z. *Anorg. Allg. Chem.* **1989**, *579*, 47.

(39) Sadler, J. L.; Bard, A. J. *J. Am. Chem. Soc.* **1968**, *90*, 1979.

Contribution from the Chemistry Division, Argonne National Laboratory, Argonne, Illinois 60439, and Chemical Technology Division, Oak Ridge National Laboratory, Oak Ridge, Tennessee 37831-6268

## Plutonium(IV) Polymers in Aqueous and Organic Media

P. Thiyagarajan,\*† H. Diamond,† L. Soderholm,† E. P. Horwitz,† L. M. Toth,† and L. K. Felker†

Received January 11, 1989

The structures of Pu(IV) hydrous polymers were measured by small-angle neutron scattering (SANS) in aqueous media and after solvent extraction in organic phases. The scattering data from polymers occurring as aqueous colloidal suspensions indicate long, thin, rodlike particles. Pu(IV) hydrous polymers formed in the presence of uranium were shorter than those produced in the absence of uranium; this is consistent with earlier observations that uranium reduces the rate of Pu(IV) polymer formation. The Pu(IV) polymers were extracted into  $\text{C}_6\text{D}_6$  solutions by alkyl esters of phosphoric acid. The extractant-Pu polymer geometries were shorter than those in the aqueous media; their radii were increased by the lengths of the extended alkyl substituents of the extractants. Comparable extractions of Pu(IV) monomers were also examined. X-ray scattering measurements exhibit well-defined Bragg diffraction lines for the Pu polymer in both the aqueous and organic phases. All of the lines could be identified with those of  $\text{PuO}_2$ . Spectrophotometric measurements monitored the polymeric nature of the aqueous and organic suspensions.

### Introduction

The hydrolysis of metal cations has been a subject of interest in numerous reports. The text by Baes and Mesmer<sup>1</sup> summarizes the status of the work up to the present decade and demonstrates the extensiveness of this phenomenon across the periodic table. As many of these metal cations hydrolyze, there is often a tendency for them to aggregate through hydroxyl bridges and form simple dimers and trimers (such as with the uranyl ion)<sup>2</sup> or extensive polymeric networks, which can reach colloidal dimensions and exist as colloidal suspensions. As metastable species, these exhibit varying degrees of stability, but often with time or at elevated temperatures, they condense (with the associated loss of water) or otherwise undergo a conversion from hydroxyl-bridged to oxygen-bridged polymeric species. This chemistry (which includes the behavior of the free metal ion and the extensively oxide-bridged polymeric aggregate) has been studied in various stages and is

summarized in texts such as that by Gimblett,<sup>2</sup> which establishes that these hydrous polymers, either hydroxyl- or oxy-bridged, are a commonly occurring phenomenon observed in many systems.

Ultimately, the stable metal oxide can be produced by precipitation of the hydrous polymer and further drying. Indeed, many reprocessing operations utilize this chemistry to produce the pure oxides. However, if the desire is to keep the metal cation in solution at a relatively high pH (e.g., for maximizing liquid/liquid extraction coefficients under some conditions), one is often confronted with the unwanted hydrolysis/polymerization side reaction. Within this scheme, the polymeric form of the hydrolyzed cation (regardless of whether it is a hydroxide-bridged or an oxygen-bridged polymer species, a simple species, or a

\* Argonne National Laboratory.

† Oak Ridge National Laboratory.

(1) Baes, C. F., Jr.; Mesmer, R. E. *Hydrolysis of Cations*; Wiley: New York, 1976; pp 187-9.

(2) Gimblett, F. G. R. *Inorganic Polymer Chemistry*; Butterworths: London, 1963.

(3) Toth, L. M.; Friedman, H. A.; Begun, G. M.; Dorris, S. E. *J. Phys. Chem.* **1984**, *88*, 5574.

complex colloidal network) compromises the reprocessing procedure. (This is usually manifested as reduced separation factors or the formation of unwanted precipitates.) As a result, considerable attention has been focused on understanding and controlling the formation of these hydrous polymers.

Viewed by others, the specific oxide-bridged stage in hydrous polymer chemistry is considered as merely metal oxide or colloid chemistry, but taken in the above context, it falls within a broader terminology. The hydrolysis of cations such as  $Zr^{4+}$ ,  $Th^{4+}$ , and  $Pu^{4+}$  has concerned reprocessing chemists for several years, and it is the later stages of plutonium hydrolytic chemistry that is the subject of this paper. Although our major interest is often with the initial stages of hydrolysis and aggregation, here we have studied the later stages prior to precipitation in order to apply small-angle scattering techniques at the most convenient point and then attempt to work forward from there to earlier stages of the chemistry.

As  $Pu^{4+}$  hydrolyzes,<sup>4</sup> it forms a wide variety of hydrous polymeric species that persist in the aqueous medium.<sup>1-3,5-9</sup> These polymers can cause problems in spent fuel and nuclear waste process schemes because they do not behave chemically as monomeric plutonium in ion-exchange and solvent extraction procedures.

The nature of the Pu(IV) polymer is highly dependent upon the conditions of formation. Freshly prepared polymers held at room temperature can be readily depolymerized, and their properties change on a time scale of hours. Polymers that have been aged for long periods at room temperature or that have been heated can remain stable for months. Only the latter polymers are considered here.

Earlier work<sup>8</sup> has shown that the presence of uranium in a polymerizing Pu(IV) solution reduces the rate of polymer formation without appreciably entering the polymer. Raman studies<sup>3,10</sup> have shown a change in the U-O stretching frequency when uranium is present during the formation of similar Th(IV) polymers and suggest that  $UO_2^{2+}$  functions as a chain terminator through the formation of hydroxy bridges to terminal uranyl groups.

The solvent extraction of Pu(IV) polymers, which can be of significance in spent fuel processing, has been reported by Ochendon and Welch<sup>9</sup> using spectrophotometry and by Muscatello, Navratil, and Killion<sup>11</sup> using spectrophotometry and distribution ratios to establish the polymeric nature of the extracted species. Early scoping studies by Peppard and Mason<sup>12</sup> used distribution ratios to establish the extraction of freshly made polymers.

We examined hydrous polymers in a state where they were stable and controllable, i.e., the aged colloidal oxide dispersed in liquid media. Within this relatively simple situation, we wished (1) to determine the particle morphology of some Pu(IV) polymers in aqueous and organic phases by using small-angle neutron scattering (SANS), spectrophotometry, and X-ray diffraction, (2) to compare the morphologies of aqueous plutonium polymer suspensions prepared in the presence and in the absence of uranium, and (3) to validate that Pu polymer can be extracted into nonaqueous media by using organophosphorus extractants.

Small-angle neutron scattering lends itself to the study of Pu polymers. SANS can give particle sizes and shapes in the range of 10 Å to a few thousand, which is the size range of Pu(IV) polymers. The technique is appropriate for both aqueous and organic media because the contrast between solvent and polymer can be easily changed by varying the hydrogen/deuterium ratio in the solvent.

X-ray and electron diffraction measurements have shown a similarity between dried Pu(IV) polymer samples and  $PuO_2$  crystalline structure.<sup>13-15</sup> These measurements are extended to both organic and aqueous liquids to establish the nature of the dispersed polymeric species.

### Experimental Section

**A. Preparation of Plutonium Polymers.** The plutonium was  $^{242}Pu$ , unless otherwise noted. The preparations used in this work all shared the features of obtaining the Pu(IV) in a pH = 1.3–1.4 nitric acid solution and heating to 85–95 °C in a container that restricted access to air. Disproportionation of the Pu(IV) ( $3Pu^{4+} + 2H_2O \rightleftharpoons PuO_2^{2+} + 2Pu^{3+} + 4H^+$ ) competed with polymer formation under these conditions,<sup>6</sup> but since the reverse reaction occurred readily, the polymer formed nearly quantitatively. Where the formation of polymer was not complete, Pu(VI) was identified by spectrophotometric measurements, and the addition of nitrite reduced the Pu(VI) to Pu(IV) and drove the polymerization to completion.

A 0.12 M Pu(IV) solution was polymerized in  $D_2O$  by heating for 7 h. After addition of nitrite, it was heated again for 6 h (sample 1).

Because the  $D_2O$  preparation (sample 1) yielded no appreciable SANS signal, further preparations were made in  $H_2O$ . A second sample, 0.09 M plutonium, was prepared by aging a  $H_2O$ - $HNO_3$  solution (pH = 1.3) of Pu(IV) for 70 h, heating for 8 h at 95 °C, adding  $NaNO_2$ , allowing the mixture to stand overnight, and heating for 6 h (sample 2).

Two samples were prepared for studying the influence of uranium on Pu(IV) polymerization. Crystals of  $^{239}Pu(NO_3)_4 \cdot 5H_2O$  were dissolved in water to make  $[Pu] = 0.093$  M. Uranyl nitrate was added to half of this solution, obtaining a U/Pu ratio of 2, and the pH was adjusted to 1.3 by using NaOH; the solution was heated at 85 °C for 24 h. The final pH of this solution was 1.08 (sample 3). The other half of the solution was subjected to similar treatment, except that the uranyl nitrate was added after the polymerization (sample 4). A third sample containing 0.093 M Pu(IV) monomer (i.e., unhydrolyzed) in 1 M  $HNO_3$  and 0.186 M uranyl nitrate served as the background in the SANS measurements of samples 3 and 4.

The Pu(IV) polymers in the organic phase were prepared as follows. A portion of sample 1 was equilibrated with 0.2 F HDHoEP (bis(hexoxyethyl) hydrogen phosphate) in  $C_6D_6$ . (We use F, the formula molecular weight, to describe the concentration of plutonium or extractant, reserving the use of M, molarity, to indicate the concentration of independent molecules.) Two-thirds of the plutonium was extracted, and some interfacial scum was observed. The clear organic phase containing 0.05 F plutonium was measured by SANS (sample 5). The effect of the extractant/Pu polymer ratio on the structure of the extracted species was examined by using a second polymer-HDHoEP preparation in  $C_6D_6$  containing 0.026 F plutonium and 0.2 F HDHoEP (sample 6). To understand the effect of varying the extractant on the morphology of the extracted polymeric species, Pu(IV) polymer (0.02 F Pu) was also extracted from the  $D_2O$  solution into 0.20 F  $H_2MEHP$  (2-ethylhexyl dihydrogen phosphate)- $C_6D_6$  (sample 9).

In parallel experiments, Pu(IV) monomer was extracted from 1 M  $HNO_3$  into 0.20 F HDHoEP- $C_6D_6$  solution: the concentration of Pu was 0.012 F (sample 7). A less concentrated solution of monomeric Pu(IV), 0.006 F, was also prepared with 0.20 F HDHoEP- $C_6D_6$  solution (sample 8). Another organic solution was prepared by extraction of monomeric Pu(IV) from 1 M  $HNO_3$  into 0.20 F  $H_2MEHP$ - $C_6D_6$  solution so that the resulting  $[Pu(IV)] = 0.03$  M (sample 10).

**B. SANS Measurements.** The samples were loaded into Suprasil cells, with 1- or 2-mm path lengths. These were sealed with Teflon stoppers and foils and further enclosed in a steel capsule with 0.05-mm vanadium windows. SANS data were measured by using the small-angle diffractometer (SAD) at the Intense Pulsed Neutron Source (IPNS) at Argonne National Laboratory. The details of this instrument and the data reduction have been described earlier.<sup>16</sup> The scattering data were cor-

(4) We shall use the standard convention here with the oxidation state of the element identified with Roman numerals, since various species can often exist, or the particular species identified with Arabic numerals, Pu(IV) or  $Pu^{4+}$ , respectively.

(5) Cleveland, J. M. *The Chemistry of Plutonium*; American Nuclear Society: La Grange Park, IL, 1979; pp 83–89 and earlier references therein.

(6) Constanzo, D. A.; Biggers, R. E.; Bell, J. T. *J. Inorg. Nucl. Chem.* **1973**, *35*, 609.

(7) Bell, J. T.; Coleman, C. F.; Constanzo, D. A.; Biggers, R. E. *J. Inorg. Nucl. Chem.* **1973**, *35*, 623.

(8) Toth, L. M.; Friedman, H. A.; Osborne, M. M. *J. Inorg. Nucl. Chem.* **1981**, *43*, 2929.

(9) Ochendon, D. W.; Welch, G. A. *J. Chem. Soc.* **1956**, 3358.

(10) Sherrow, S. A.; Toth, L. M.; Begun, G. M. *Inorg. Chem.* **1986**, *25*, 1992.

(11) Muscatello, A. C.; Navratil, J. D.; Killion, M. E. *Sep. Sci. Technol.* **1983**, *18*, 1731.

(12) Peppard, D. F.; Mason, G. W. Private communication.

(13) Lloyd, M. H.; Haire, R. G. *Radiochim. Acta* **1978**, *25*, 139.

(14) Haire, R. G.; Lloyd, M. H.; Beasley, M. L.; Mulligan, W. O. *J. Electron. Microsc.* **1971**, *20*, 8.

(15) Lloyd, M. H.; Tallent, O. K. *Nucl. Technol.* **1973**, *18*, 205.

(16) Epperson, J. E.; Thyagarajan, P.; Klippert, T. E. *SAD Manual*; Argonne National Laboratory: Argonne, IL, 1988.

**Table I.** Dimensions of Plutonium Polymers in Solution

sample no.	description	modified Guinier diameter, Å	ellipsoidal model		$\chi^2/DF^c$
			diameter, Å <sup>a</sup>	length, Å <sup>b</sup>	
1	Pu(IV) polymer in D <sub>2</sub> O	<i>e</i>	<i>e</i>	<i>e</i>	
2	Pu(IV) polymer in H <sub>2</sub> O	46 ± 2	47 ± 2	>1900	2.0
3	Pu(IV) polymerized in presence of U(VI)		25 ± 6	84 ± 14	0.8
4	Pu(IV) polymerized and U(VI) added later		22 ± 3	120 ± 10	0.7
5	HDHoEP/Pu polymer = 4	74 ± 1	73 ± 2	214 ± 6	1.7
6	HDHoEP/Pu polymer = 8	65 ± 1	70 ± 2	248 ± 16	0.9
7	HDHoEP/Pu monomer = 8 <sup>d</sup>	34 ± 1	37 ± 4	1000 ± 200	6
8	HDHoEP/Pu monomer = 16 <sup>d</sup>		10 ± 2	58 ± 4	1
9	H <sub>2</sub> MEHP/Pu polymer = 10	75 ± 2	78 ± 4	370 ± 80	1.3
10	H <sub>2</sub> MEHP/Pu monomer = 7 <sup>d</sup>		6 ± 4	58 ± 2	1.0

<sup>a</sup>Twice the value of *a* for eq 1. <sup>b</sup>Twice the value of the *b* for eq 1. <sup>c</sup>DF = degrees of freedom. <sup>d</sup>This is a polymer of a different sort (see text). <sup>e</sup>Not discernible by SANS.

rected for the empty cell scattering, transmission, integrated beam intensity, and detector efficiency. All the scattering data were placed on an absolute scale by using a 50:50 v/v polymer melt sample of perdeuterated and hydrogenated polystyrene, whose absolute scattering cross section was available from measurements at the 30-m SANS instrument at Oak Ridge National Laboratory.<sup>17</sup>

**C. Visible Spectrometry.** The polymeric nature of each sample was validated by its spectrum from 370 to 1300 nm. Pu(IV) polymer exhibited a very high absorption coefficient at 400 nm (nominally, 150 L/(mol cm), based upon the individual plutonium atom concentration). The absence of Pu(III), monomeric Pu(IV), Pu(V), and Pu(VI) monomers could be established by inspection of the spectra.<sup>6</sup> The Pu(IV) polymer concentrations were established by using  $\alpha$ -pulse analyses and spectrophotometry.

**D. X-ray Diffraction.** The Pu polymer liquid samples in 0.7-mm Lindemann tubes were measured by using the Debye-Scherrer geometry, Cu K $\alpha$  radiation (1.54188 Å), and a photographic film detector. The lines were read from the film visually.

## Results and Interpretation

**A. Pu(IV) Polymer in Water.** The H<sub>2</sub>O preparation of Pu(IV) polymer (sample 2) formed elongated particles. This is apparent (Figure 1a) from the slope close to unity in the log-log plot of the intensity (*I*) of scattered neutrons vs  $Q = (4\pi/\lambda) \sin \theta$ ;  $\lambda$  is the neutron wavelength, and  $2\theta$  is the neutron scattering angle. More explicitly, a modified Guinier plot [ $\ln(QI)$  vs  $Q^2$ ] of the data (Figure 1b) exhibits a linear region, whose slope gives the cross-sectional radius of gyration ( $R_c$ ).

The length of the Pu polymer (from the radius of gyration  $R_g$ ) in H<sub>2</sub>O could not readily be obtained from a Guinier analysis ( $\ln I$  vs  $Q^2$ ) since no linearity was seen in the low- $Q$  region. This absence of linearity could be due to the presence of very long particles or polydispersity.

Further analyses compared the data to the response expected from a uniform assemblage of cylinders<sup>18</sup> or ellipsoids of revolution<sup>18</sup> that were oriented at random to the incident neutron beam. The results from the two models were similar, but the ellipsoids of revolution had a wider range of applicability for systems with various length-to-diameter ratios. Other models (spheres, random coils) did not fit the data well.

The neutron-scattering pattern for each sample was fitted by using the model expressed in eq 1 (i.e., the scattering from ellipsoids of revolution), and the results are summarized in Table I. In eq 1  $X = Qa[\cos^2 \beta + (b/a)^2 \sin^2 \beta]^{1/2}$ , *a* and *b* are the

$$I(Q) = I(0) \int_0^{\pi/2} [3(\sin X - X \cos X)/X^3]^2 \cos \beta \, d\beta + B \quad (1)$$

minor and major semiaxes of the ellipsoid,  $I(0)$  is the extrapolated ( $Q = 0$ ) intensity of the coherently scattered neutrons, and *B* is the incoherent background. The integral takes into account all orientations of the ellipsoid. The background subtraction for each data set used the (normalized) signal from a comparable solution that contained no polymer. Thus the background was set to zero.

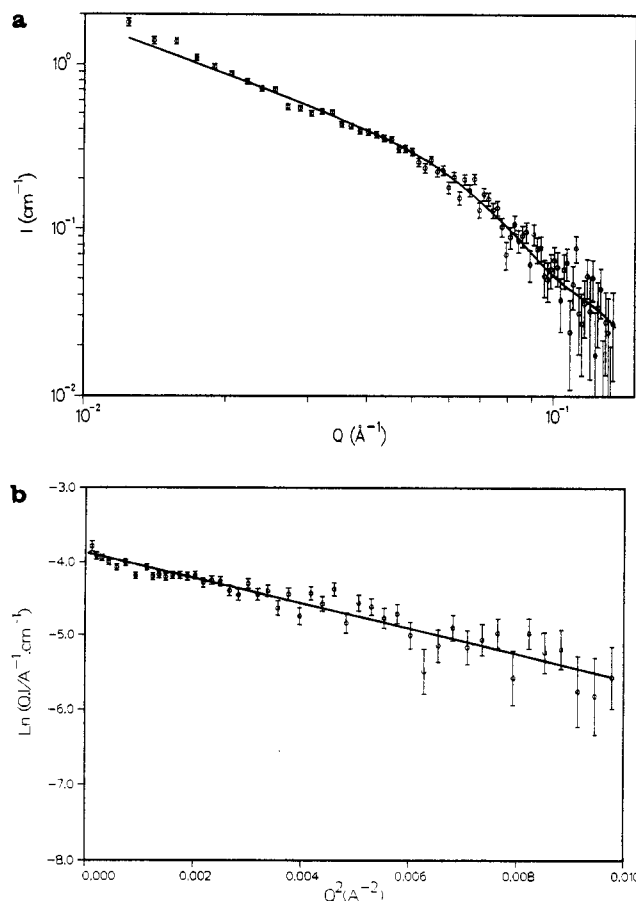


**Figure 1.** (a) SANS data for the Pu(IV) polymer in H<sub>2</sub>O (sample 2). The solid line is calculated from eq 1 by using length and diameter from Table I. (b) Modified Guinier plot for the sample in (a).

Independent analyses in which *B* was adjustable supported this approach. For simplicity, we express the particle sizes as total length and diameter of the ellipsoids of revolution.

Figure 1a shows a plot of the data for sample 2, Pu(IV) polymer in water, and their correspondence to eq 1. The calculated curve satisfactorily agrees with the experimental data in the region  $Q = 0.015$ – $0.15 \text{ Å}^{-1}$ , yielding a length of  $1900 \pm 200 \text{ Å}$  and a diameter of  $47 \pm 2 \text{ Å}$ . This diameter agrees well with that obtained from the modified Guinier analysis (Figure 1b) for long, thin particles,<sup>19</sup> which gives a cross-sectional radius of gyration ( $R_c$ ) of  $17 \pm 1 \text{ Å}$  and a corresponding diameter of  $48 \pm 3 \text{ Å}$ . It is seen in Figure 1a that the data below  $Q = 0.015 \text{ Å}^{-1}$  deviates upward from the calculated curve, suggesting the presence of particles longer than 1900 Å. The length could not be determined, and hence the calculated length should be taken as a lower limit.

(17) Bates, F. S.; Wignall, G. D. *Macromolecules* **1986**, *19*, 934.

(18) Guinier, A.; Fournet, G. *Small Angle Scattering of X-rays*; Walker, C. B. (translator), Yudowitch, K. L. (compiler); Wiley: New York, 1955; p 19, eqs 31, 32.

(19) Porod, G. In *Small Angle X-ray Scattering*; Glatter, O., Kratky, O., Eds.; Academic Press: New York, 1982; Chapter 2, eq 52.

**Table II.** Observed<sup>a</sup> *d* Spacings for Pu(IV) Polymer Solutions from X-ray Diffraction

<i>hkl</i>	PuO <sub>2</sub> <sup>b</sup>	sample			
		1	2 <sup>c</sup>	4	5
111	3.08	3.20	3.14	3.07	
200	2.67	2.70	2.72		
220	1.894	1.90	1.92	1.895	1.94
311	1.617	1.65	1.63	1.60	1.64
222	1.548				
331	1.234	1.23	1.23		1.23
420	1.203				
422	1.100	1.11	1.11		
511/333	1.037		0.98		

<sup>a</sup> Line positions reported represent the line center in angstroms.

<sup>b</sup> From ref 20. <sup>c</sup> These data were used to obtain a least-squares fit to a cubic lattice constant of 5.398 ± 0.015 Å.

X-ray diffraction lines, obtained for the Pu(IV) polymers in H<sub>2</sub>O and D<sub>2</sub>O are given in Table II. The *d* spacings resemble those reported for dried Pu(IV) polymer<sup>13-15</sup> and for crystalline PuO<sub>2</sub>.<sup>20</sup> Crystalline PuO<sub>2</sub> is a CaF<sub>2</sub>-type face-centered cubic structure in which each plutonium atom is surrounded by eight equidistant oxygen atoms. The cell constant calculated for sample 2 (in H<sub>2</sub>O) is 5.398 ± 0.015 Å (compared to 5.3960 Å for PuO<sub>2</sub>).<sup>20</sup> If the density of plutonium atoms in Pu(IV) polymer dispersed in water were the same as that of its crystalline analogue, then the number of plutonium atoms that would fit into the polymer volume determined from SANS is about 50 000. Further, if the composition of the polymer were the same as the crystalline material, the scattering length density for SANS would be 5.015 × 10<sup>10</sup> cm<sup>-2</sup>. This would explain the very weak SANS signal found in D<sub>2</sub>O (6.36 × 10<sup>10</sup> cm<sup>-2</sup>), which offered little contrast, and the strong signal observed in H<sub>2</sub>O (-0.55 × 10<sup>10</sup> cm<sup>-2</sup>).

As the ordering in a crystalline lattice becomes less than 10<sup>3</sup> Å, the X-ray lines broaden according to<sup>21</sup>

$$W = 0.9\lambda / (S \cos \theta) \quad (2)$$

where *W* is the full width at half-height in radians,  $\lambda$  is the X-ray wavelength,  $\theta$  is the Bragg angle, and *S* is the minimum dimension of the ordered lattice. The observed minimum dimension from eq 2 is 60 ± 15 Å for polymers in aqueous suspension (samples 1 and 2, Table II). This is consistent with the diameter determined by SANS for sample 2 of 47 ± 2 Å.

A dependence of line width on the order of reflection would give an indication of line broadening due to crystal defects.<sup>21b</sup> From our limited data, no such dependence is seen, so the observed broadening can be identified with the finite size of the particles rather than with crystal defects.

**B. Pu Polymer Prepared in the Presence and Absence of Uranium.** Figure 2 shows the SANS response for Pu polymer samples prepared in the same way, except that uranium was present initially in sample 3 and it was added after polymerization in sample 4. The ellipsoidal-model calculations (Table I) show that sample 4 is longer than sample 3; their diameters are similar. That the particle size is smaller for sample 3 can be seen by observing the signal intensities at  $Q = 0$ , [*I*(0)], whether determined from eq 1 or from extrapolated Guinier plots. The *I*(0), which is proportional to the product of the particle volume squared and the particle concentration, is about twice as great for sample 4 as for sample 3.

The observed difference conforms to predictions based upon measurements<sup>8</sup> of initial Pu polymerization rates in the presence and absence of uranium. In this work we see that the polymers are elongated and the presence of uranium during polymer formation reduces the length.

The U/Pu = 2 ratio employed here is smaller than in the earlier work<sup>8</sup> (U/Pu = 10) because the polymer would have precipitated

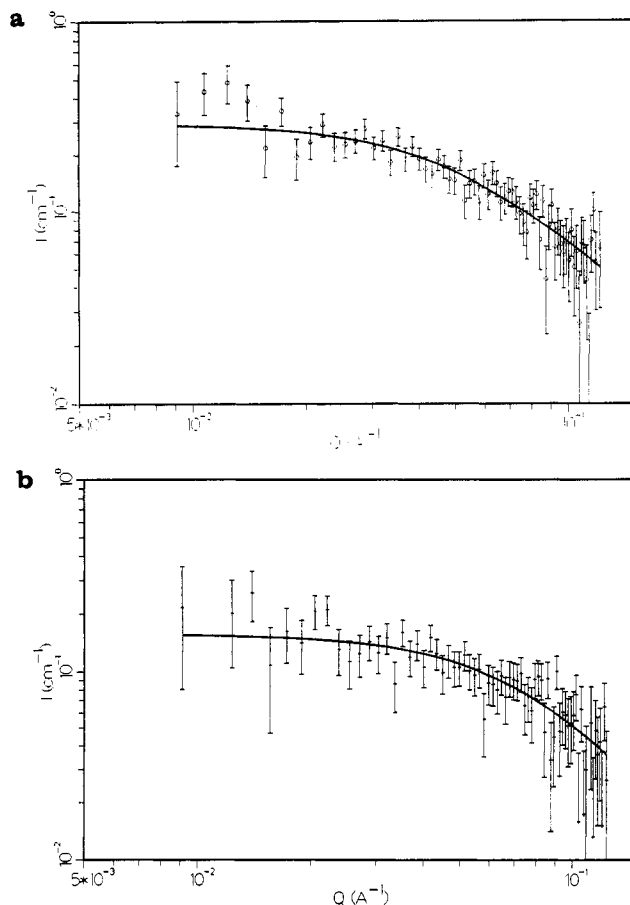


**Figure 2.** (a) SANS data for the plutonium polymer (sample 4) prepared in the absence of uranium; uranium added later. (b) SANS data for the plutonium polymer (sample 3) prepared as in a, except that uranium was present during polymerization. Solid lines correspond to eq 1, for dimensions in Table I.

in the presence of large amounts of UO<sub>2</sub>(NO<sub>3</sub>)<sub>2</sub>.<sup>22</sup> The difference in size observed here would be expected to be larger if more uranium could be used.

**C. Pu Polymer in Nonaqueous Media.** The extractants, HDHoEP (bis(hexoxyethyl) hydrogen phosphate) and H<sub>2</sub>MEHP (2-ethylhexyl dihydrogen phosphate), extract the very large Pu(IV) polymers, as evidenced by the disappearance of all plutonium color from the aqueous phase when there is a sufficient excess of extractant. The extracted species in the organic phase is still polymeric, as seen by the characteristically high spectrophotometric absorption at 400 nm and by the absence of the Pu(IV) monomer peak near 476 nm. Visually, the characteristic polymer color is preserved; the color passes from the aqueous to the organic phase in less than 1 min at room temperature. When there is an excess of Pu(IV) polymer, an interfacial solid is formed.

In the C<sub>6</sub>D<sub>6</sub> dispersion of the extracted Pu polymer, the SANS is most sensitive to the highly contrasted hydrogen atoms of the alkyl chains of the phosphoric acid esters. The scattering data and the fitted-model results are shown for HDHoEP and H<sub>2</sub>MEHP in Figure 3. The diameters of the ellipsoids of the extractant-Pu(IV) polymer complexes in C<sub>6</sub>D<sub>6</sub> (samples 5, 6, and 9 and Table I) are quite similar for both extractants, about 26 Å larger than that of an aqueous polymer. Modified Guinier analyses (Figure 3a) also yield similar cross-sectional dimensions. This increase in diameter is just what one would expect if the HDHoEP or H<sub>2</sub>MEHP molecules are attached around the rod-shaped Pu polymer. Both HDHoEP and H<sub>2</sub>MEHP extend about 13 Å from the farthest reach of the alkyl group to the phosphate portion of the molecule.<sup>23</sup> The placement of the extractant

(20) Asprey, L. B.; Ellenger, F. H.; Fried, S.; Zachariasen, W. H. *J. Am. Chem. Soc.* **1955**, *77*, 1707.

(21) (a) P. Scherrer *Goettinger Nachr.* **1918**, *2*, 98. (b) Guinier, A. *X-Ray Diffraction*; W. H. Freeman and Co.: San Francisco, 1963; Chapters 5 and 6.

(22) Bell, J. T.; Coleman, C. F.; Constanzo, D. A.; Biggers, R. E. *J. Inorg. Nucl. Chem.* **1973**, *35*, 629.

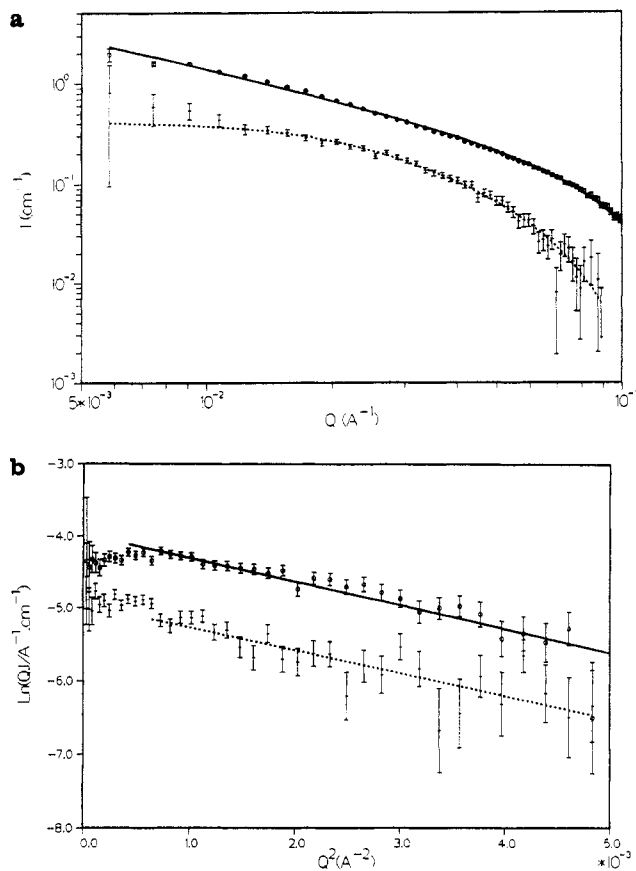


**Figure 3.** (a) SANS data for Pu(IV) polymer extracted into deuterio-benzene solutions of  $\text{H}_2\text{MEHP}$  (upper curve, sample 9) and HDHoEP (lower curve, sample 6) along with eq 1 fit. (b) Modified Guinier plots and fitted lines for Pu(IV) polymer extracted by  $\text{H}_2\text{MEHP}$  (upper curve, sample 9) and HDHoEP (lower curve, sample 6).

molecules around the polymer with their hydrophobic tails pointed outward changes the polymer from a hydrophilic to a lipophilic species and thus solvates the particles in  $\text{C}_6\text{D}_6$ . The lengths of these extracted particles are shorter than the length of the particles in the aqueous phase. This can also be seen by comparing the curvatures in the low- $Q$  region of the modified Guinier plots for the aqueous (Figure 1b) and the organic (Figure 3b) dispersions. In the case of the longer aqueous polymer, there is no apparent downward curvature and the organic phase polymers show marked downward curvatures.

The X-ray diffraction pattern of the  $\text{C}_6\text{D}_6$  solution (sample 5) of HDHoEP-Pu(IV) polymer contains diffuse lines corresponding (Table II) to those of crystalline  $\text{PuO}_2$ . Thus, there is additional strong evidence for the maintenance of the integrity of the polymer as it crosses the phase boundary, albeit that its longitudinal dimension is shortened by extraction. Small crystalline  $\text{CeO}_2$  particles have been stabilized in organic solutions by long-chain carboxylic acids.<sup>24</sup>

In parallel experiments, Pu(IV) monomer was extracted from 1 M  $\text{HNO}_3$  into  $\text{C}_6\text{D}_6$  solutions of each of the extractants. This was done to study the difference between extracted monomeric and polymeric species. SANS data are shown for two different HDHoEP/Pu ratios for Pu polymeric (Figure 4a) and for Pu monomeric (Figure 4b) extracted species. A large polymer was observed upon extraction of Pu(IV) monomer when the HDHoEP/Pu ratio was 8 (sample 7), but the particle size was quite small when the ratio was doubled to 16 (sample 8). In contrast to these observations, there was little change in the sizes of the extracted Pu polymeric species when the HDHoEP/Pu ratio was more than doubled (Figure 4a, Table I). The Pu monomer

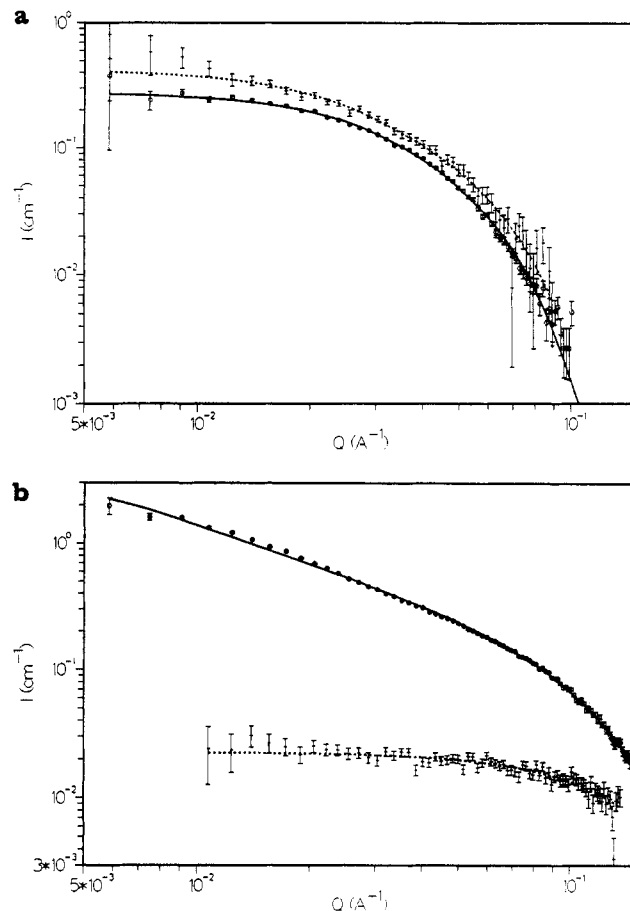


**Figure 4.** Effect of extractant/Pu ratio on the two types of polymers, showing the SANS data and fits to eq 1: (a) HDHoEP/Pu(IV) polymer samples 5 (—) and 6 (---); (b) HDHoEP/Pu(IV) monomer samples 7 (—) and 8 (---). The extractant/Pu ratio has profound effect on the particle sizes of extracted monomers and little effect on the extracted polymers.

extracted by  $\text{H}_2\text{MEHP}$  did not polymerize much since the  $\text{H}_2\text{MEHP}/\text{Pu}$  ratio was 16.

The optical absorption coefficient for both monomeric extracted samples at 400 nm was less than 8 L/(mol cm) (19-fold less than that of the polymer resulting from hydrolysis), and the Pu(IV) monomer peak at 480 nm was dominant. The natures of polymers formed by the extracted Pu(IV) monomeric and extracted Pu(IV) polymeric species are quite different. Polymer formation by divalent and trivalent metal ions and acidic organophosphorus extractants is a well-known phenomenon<sup>25</sup> that occurs at low extractant/metal ratios. The O-P-O group of the phosphate extractant serves as a bridging agent to form long and thin chains -O-M-O-P-O-M-O-, where M is a metal. The extracted Pu monomeric species forms a polymer of this type. Where the HDHoEP/Pu monomer ratio was doubled, the size of the particles was greatly reduced, as expected from the known<sup>26</sup> chain-terminating properties of excess extractant in this type of polymer.

### Conclusions

The minimum  $Q$  value available for these measurements (about  $0.008 \text{ \AA}^{-1}$ ) makes it difficult to accurately determine the particle dimensions of 1000  $\text{\AA}$  and longer. Furthermore, the polydispersity that may be present in the lengths and (perhaps) in the diameters of the particles limits the amount of geometrical information that can be extracted from SANS data. However, the good conformity of the scattering data to that expected from the hypothetical models (and the poor conformity to alternative models) give unambiguous evidence that the Pu(IV) polymers exist as elongated

(23) Gatrone, R. C. Private communication, 1988.

(24) Brittain, H. G.; Grateff, P. S. *J. Less-Common Met.* **1983**, *94*, 277.

(25) Thiyagarajan, P.; Diamond, H.; Danesi, P. R.; Horwitz, E. P. *Inorg. Chem.* **1987**, *26*, 4209.

(26) Kolarik, Z.; Grimm, R. *J. Inorg. Nucl. Chem.* **1976**, *38*, 1721.

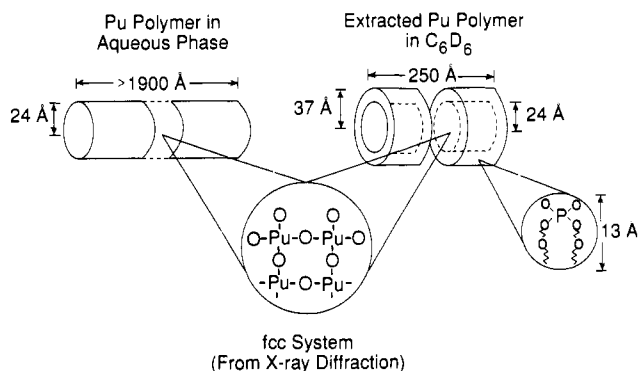


**Figure 5.** Schematic representation of a model for the observed Pu(IV) polymer.

particles in aqueous media. This differs from electron microscope findings<sup>13,14</sup> for other preparations of the polymer. The method of preparation may influence the morphology of polymers. All of the polymers studied share the same general shape, but those subjected to less heating were smaller in each dimension.

When uranium is present during polymerization of Pu(IV), shorter particles are formed than Pu(IV) polymer particles polymerized under the same conditions in the absence of uranium. The evidence supports earlier work<sup>8</sup> in which uranium was ob-

served to inhibit the rate of Pu(IV) polymerization.

Although polymers have been extracted by HDHoEP, H<sub>2</sub>MEHP, and other extractants previously,<sup>12</sup> the work was preliminary and involved only freshly prepared polymers. Here we report very large particles being extracted into deuteriobenzene solutions, preserving their highly ordered structure as shown by X-ray diffraction. In the process of extraction, the polymers are broken into shorter pieces, while the cross section of the polymeric core is preserved. Figure 5 provides a schematic representation of the structure of Pu(IV) polymers emerging from these studies.

An entirely different kind of polymer is formed upon extraction of the plutonium monomer by HDHoEP and H<sub>2</sub>MEHP. Unlike those of the extracted species of hydrolytically formed Pu polymer, the sizes of these particles depend upon the extractant/Pu ratio and their optical spectra retain Pu(IV) monomer features.

**Acknowledgment.** We thank R. C. Gatrone for calculating the minimum-energy conformations of the extractant molecules, E. Epperson for helpful discussions and provision of computer programs, T. E. Klippert for experimental support, and J. Gregar for producing quartz cells. G. W. Mason synthesized HDHoEP and H<sub>2</sub>MEHP. The Intense Pulsed Neutron Source at Argonne National Laboratory is funded by BES-Materials Science, U.S. Department of Energy, under Contract W-31-109-ENG-38.

**Registry No.** Pu, 7440-07-5; U, 7440-61-1; bis(2-(hexyloxy)ethyl) phosphate, 3538-36-1; mono(2-ethylhexyl) phosphate, 1070-03-7.

Contribution from the Department of Physical and Life Sciences, University of Portland, Portland, Oregon 97203, and Department of Chemical and Biological Sciences, Oregon Graduate Institute of Science & Technology, Beaverton, Oregon 97006-1999

## Chemistry and Electronic and Vibrational Spectroscopy of Mononuclear and Dinuclear (Tris(1-pyrazolyl)borato)- and Chloromolybdenum(V)-Oxo Complexes

Sandra E. Lincoln\*<sup>†</sup> and Thomas M. Loehr<sup>†</sup>

Received October 16, 1989

Hydrolysis of the Mo(V) complex  $\text{HB}(\text{pz})_3\text{MoOCl}_2$  leads to two geometric isomers of formula  $[\text{HB}(\text{pz})_3\text{MoOCl}]_2\text{O}$  (**2**). Crystal structures (Lincoln, S.; Koch, S. A. *Inorg. Chem.* **1986**, *25*, 1594-1602) show them to be linear  $\mu$ -oxo-bridged Mo-O-Mo complexes. **2a** has a pseudo 2-fold axis of symmetry through the  $\mu$ -oxo atom with respect to the chloro ligands, whereas **2b** is centrosymmetric with molecular and crystallographic  $C_i$  symmetry. Both dinuclear complexes exhibit an intense absorption at 462 nm ( $\epsilon \geq 9000 \text{ M}^{-1} \text{ cm}^{-1}$ ). In the present study, infrared and (resonance) Raman experiments have been carried out to test the symmetry dependence of bands associated with the Mo-O-Mo bridge. Both of the dinuclear compounds possess very intense bands at  $\sim 380 \text{ cm}^{-1}$ , identified for the first time as the symmetric stretch,  $\nu_s(\text{Mo-O-Mo})$ , of  $\text{Mo}_2\text{O}_3^{4+}$  complexes. The excitation profile of this mode tracks the 462-nm absorption, identifying it as a charge-transfer transition of the Mo-O-Mo group. The strong IR band at  $\sim 460 \text{ cm}^{-1}$  is also intense in the Raman spectrum of **2a** but weak for **2b**. It has been identified as the bridge deformation mode of the  $\text{Mo}_2\text{O}_3^{4+}$  unit. The resonance Raman spectra of both complexes show strong overtone and combination bands involving  $\nu_s(\text{Mo-O-Mo})$ ,  $\delta(\text{Mo-O-Mo})$ , and  $\nu_{as}(\text{Mo-O-Mo})$ . For the centrosymmetric species, these combination and overtone bands are strikingly intense because the fundamentals  $\delta$  and  $\nu_{as}$  are symmetry-forbidden vibrations. Vibrational spectroscopic assignments are supported by <sup>18</sup>O-isotope substitutions, symmetry, and intensity analyses. In addition, the dinuclear species  $[\text{Mo}_2\text{O}_3\text{Cl}_2]^{4-}$  formed in 5-6 M HCl is characterized by Raman spectroscopy, supporting the linear, or nearly linear, Mo-O-Mo structure as originally proposed (Haight, G. P. *J. Inorg. Nucl. Chem.* **1962**, *24*, 663).

### Introduction

The chemistry of Mo(V)-oxo complexes is of importance in industrial and biochemical catalysis.<sup>1-7</sup> In contrast to the intense investigation of mononuclear Mo=O compounds,<sup>2,8-13</sup> relatively little is known about the electronic spectroscopic properties of dinuclear  $\text{Mo}_2\text{O}_3^{4+}$  complexes. The hydrotris(1-pyrazolyl)borate coordination compounds  $\text{HB}(\text{pz})_3\text{MoOCl}_2$ ,  $[\text{HB}(\text{pz})_3\text{MoOCl}]_2\text{O}$ , and  $[\text{HB}(\text{pz})_3]_2\text{Mo}_2\text{O}_2(\mu\text{-O})_2$  provide an opportune system for

comparing chemical and spectral properties of mononuclear  $\text{MoO}^{3+}$  and dinuclear  $\text{Mo}_2\text{O}_3^{4+}$  complexes.

- (1) (a) Coughlan, M., Ed. *Molybdenum and Molybdenum-Containing Enzymes*; Pergamon: New York, 1980. (b) Newton, W. E.; Otsuka, S. *Molybdenum Chemistry of Biological Significance*; Plenum: New York, 1980. (c) Spiro, T. G., Ed. *Molybdenum Enzymes*; Wiley-Interscience: New York, 1986.
- (2) Stiefel, E. I. *Prog. Inorg. Chem.* **1977**, *22*, 1-223 and references therein.
- (3) Stiefel, E. I. In *Molybdenum and Molybdenum-Containing Enzymes*; Pergamon: New York, 1980; pp 41-98.
- (4) Pope, M. T.; Still, E. R.; Williams, R. J. P. In *Molybdenum and Molybdenum-Containing Enzymes*; Pergamon: New York, 1980; pp 1-40.
- (5) Spivack, B.; Dori, Z. *Coord. Chem. Rev.* **1975**, *17*, 99.

<sup>†</sup> University of Portland.

<sup>‡</sup> Oregon Graduate Institute of Science & Technology.